Japan Geoscience Union Meeting 2012
(May 20-25 2012 at Makuhari, Chiba, Japan)

STT57-01 Room:201A Time:May 23 15:30-15:45

PALSAR ScanSAR Interferometry Using The Modified Full Aperture Processing

SHIMADA, Masanobu[1*]

[1]Japan Aerospace Exploration Agency

ScanSAR processing is represented by a Specan SAR and a full aperture SAR, latter of which creates the interpolated raw data from the intermittently transmitted and received signal and zero padding based on the transmit/receive timing. Here, we propose a modified full aperture ScanSAR imaging that performs the azimuth correlation for the azimuthally resampled range compressed data using the referenced PRF-value. This method allows the creation of the full swath SLC and allows the co-registration easily in the InSAR processing. We have tested the sensitivity of the ScanSAR interferometry for various types of the targets, disaster, desert, forest, and evaluated the coherence dependence on the beam synchronization.

At the operation of the PALSAR ScanSAR imaging (amplitude), we adopted the SPECAN SAR processing algorithm for the PALSAR wide-swath (ScanSAR) imaging [1][2]. The Specan method [1] minimized the three representative problems that the ScanSAR faces, i.e., scalloping, azimuth ambiguity, and inter-scan banding. While the SPECAN algorithm exceeds the full aperture SAR processing in that no out-of-use area exists, i.e., synthetic aperture length, in the processing phase, the phase continuity over the contiguous burst seems to be difficult. The PALSAR first Specan ScanSAR-ScanSAR interferometry was tested [3]. We first compared the strip InSAR and Specan InSAR for the simulated ScanSAR from the strip. This does not generate any discontinuity between the images. Second image is the ScanSAR result for the Saharan Desert area, which shows the relatively high coherence and the very good fringe. However, the problem was the discontinuity of the fringes. Third example is the ScanSAR of the south of the Tanzania area. This also shows high coherence and good fringes. But the problem was the phase discontinuity. Thus, in this paper, we propose a modified full aperture ScanSAR processing and its application to the ScanSAR Interferometry.

Keywords: SAR, ScanSAR InSAR, Surface Deformation, ALOS

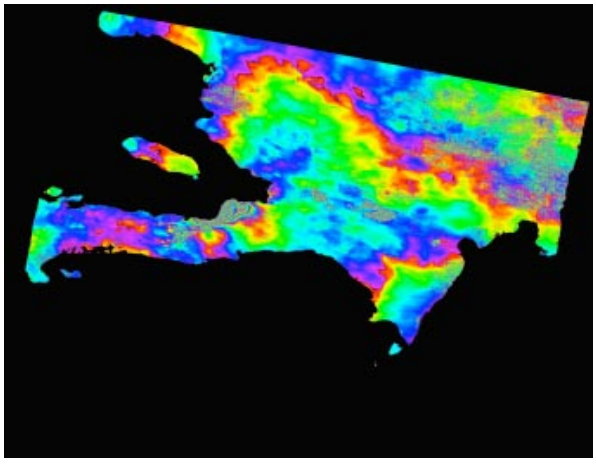

Japan Geoscience Union Meeting 2012
(May 20-25 2012 at Makuhari, Chiba, Japan)

STT57-02 Room:201A Time:May 23 15:45-16:00

Evaluation for detection capability of ground subsidence by InSAR time series analysis

MIYAHARA, Basara[1*], YAMANAKA, Masayuki[1], KOBAYASHI, Tomokazu[1]

[1]Geospatial Information Authority of Japan

Geospatial Information Authority of Japan (GSI) has been monitoring ground subsidence at 17 areas in Japan with SAR Interferometry (InSAR) analysis of ALOS/PALSAR. The subsidence is estimated by stacking process of several InSAR images, which averages and reduces noise included in the images. We evaluated detection capability of the stacking method by comparing subsidence measured by leveling. The result shows that the subsidence detected by both methods is consistent within about 1cm at Kujukuri Plain, Tsugaru Plain and Niigata Plain. In order to evaluate detection capability of ground subsidence by InSAR time series analysis, we estimate subsidence by InSAR time series analysis at still subsiding Tsugaru Plain, and compare the result with those by leveling and stacking method.

Keywords: SAR Interferometry, Time series analysis, Ground subsidence, StaMPS, ALOS, PALSAR

Japan Geoscience Union Meeting 2012
(May 20-25 2012 at Makuhari, Chiba, Japan)

STT57-03 Room:201A Time:May 23 16:00-16:15

Three dimensional water vapor distribution based on InSAR data during Seinoh heavy rain on 2 September 2008

KINOSHITA, Youhei[1*], SHIMADA, Masanobu[2], FURUYA, Masato[1]

[1]Natural History Sci. Hokkaido Univ., [2]Earth Observation Research Center, Japan Aerospace exploration Agency

Interferometric Synthetic Aperture Radar (InSAR) phase signals allow us to map the Earth's surface deformation, but are also affected by earth's atmosphere. In particular, the spatiotemporal heterogeneity of water vapor near the surface causes unpredictable phase changes in InSAR data and prevents us from detecting few centimeters of crustal deformation. However, InSAR can provide us with a spatial distribution of precipitable water vapor with unprecedented spatial resolution in the absence of deformation signals and other errors (Fujiwara et al., 1998, Hanssen et al., 1999).

We generated the InSAR image from ALOS/PALSAR level 1.0 data acquired during the heavy rain on 2 September 2008 in Central Japan, so-called Seinoh heavy rain, and then we detected the localized signal which changed 120 mm in radar line-of-sight over a spatial scale on the order of 8 km. So far we have reported that; 1) the localized signal is likely to be an artifact of tropospheric propagation delay rather than that of either ground deformation or ionosphere, 2) comparing it with the 1 km weather radar rainfall intensity echo distribution, the small area with rainfall intensity greater than 80 mm/hr exists at the location of the signal in InSAR (Kinoshita et al., GSJ 2010, 2011 meeting, Kinoshita et al., 2011, JpGU). Here we report the estimated result of three dimensional water vapor distribution during the heavy rain based on the heavy rain-derived tropospheric delay signal in InSAR data with the ray tracing method (Hobiger et al., 2008). We used the GAMMA software for the InSAR analysis and the 10 m digital elevation model by GSI for the correction of topographic fringes.

The refractivity of earth's atmosphere is the function of pressure, temperature, and water vapor (Thayer, 1974). Therefore we estimated the three dimensional water vapor distribution to explain the localized signal in InSAR by at first setting the three dimensional field of pressure, temperature and water vapor around the localized signal at the SAR acquisition time, then modeling the tropospheric delay in InSAR with ray tracing. Here, since it is impossible to determine these three parameters uniquely from one refractivity without any constraint, and since the ray path of each pixel is parallel in InSAR, it is difficult to estimate these parameters by the inversion like GPS tomography (e.g. Seko et al., 2000). For these reasons, we assumed as a constraint that the values of pressure and temperature are same as the MSM data, and we only estimated the water vapor distribution, which is spatiotemporally variable and has large effect on the propagation delay, by trial and error. In this study we focus only on the localized signal in InSAR, and the region we estimate is 30 km square centered on the localized signal in the horizontal and 15000 m in the vertical.

As a result, we estimated that there is the dry region lower than 50 % in relative humidity above 5000 m altitude, and the large amount of water vapor higher than 90 % in relative humidity within 10 km square in the horizontal and from the surface to 9000 m in the vertical at the localized signal in InSAR. Calculating the zenith precipitable water vapor (PWV) from the estimated water vapor field, we found that the amount of PWV at the signal in InSAR is 12 mm higher than that around the signal, and the location of it is 3 km apart from the local maximum area of weather radar echo. Additionally, it seems that AMeDAS surface wind observation data shows the existence of the convergence zone at the signal in InSAR. This indicates that water vapor near the surface converges at the signal. For these reasons, the location of the dense water vapor area is markedly different from that of the maximum precipitation radar echo. This observation would represent that in the precipitation system for the heavy rain the actually precipitating area was 3 km distant from the area where the water vapor was flowing into.

Keywords: InSAR, Heavy rain, Ray tracing, Water vapor

Japan Geoscience Union Meeting 2012
(May 20-25 2012 at Makuhari, Chiba, Japan)

STT57-04 Room:201A Time:May 23 16:15-16:30

Crustal deformation around 62-II crater of Tokachidake Volcano, central Hokkaido Japan, depicted by InSAR of AlOS/PALSAR

KOSHIROMARU, Takuma[1*]

[1]Inst. of Seismology and Volcanology, Hokkaido Univ.

Mt. Tokachi is an active volcano with an altitude of about 2077 m, located almost at the center of the Mt. Tokachi volcano group which aligns along northeast to southwest trend in the central Hokkaido. Since the beginning of the 20th century Mt. Tokachi has been repeating eruptions in 1926, 1962, and 1988-89 with an approximate recurrence period of 30 years. In the north-northwest part of Mt. Tokachi there are number of craters, i.e., Nokogiridake crater, Ground crater, Suribachi crater, Kita-mukai crater, Tyuoh crater, and 62-II crater. Among them the 62-II crater was formed by the eruption in 1962 and also used by eruption in 1988-1989. GPS observations by Japan metrological agency and others revealed that an inflation around this crater is on-going. In this paper, we present ALOS/PALSAR interferomety results depicting deformation of crustal deformations of Tokachi volcano.

We used ALOS/PALSAR data taken during the period from 2006 to 2010. A total of 38 scenes (20 from ascending and 18 from descending orbits) were available for the analysis. From these raw data, we constructed interferogramas for the pairs whose orbit baseline lengths are reasonably short and temporal baseline is sufficiently long. Firstly we examined only nterferograms with the highest quality. From the first analysis we excluded interferotrams where the paired observations were carried out to the snow covered ground and/or ones having large noises caused by the atomosphere. Those errors are caused by the heterogeneous microwave propagation through the ionosphere and troposphere. An example of such high-quality data was taken with the pair on June 30, 2008 and October 3, 2009. We can recognize a localized phase change pattern around 62-II crater, suggesting an localized inflation around the crater which is in good agreement with the GPS results.

Then we stacked relatively good interferograms with small noises scattering over the observed region. In many cases those noises are in good correlation of the trend of the rugged topography of the mountainous region suggesting existence of propagation heterogeneity in the data, which expected to be of random nature. The stacked interferogram also depicts a localized phase change around 62-II crater which is in good agreement with the highest quality interferograms as well as GPS data. We do not find any other significant fringes (phase changes) around the other craters. By fitting of Mogi model for our InSAR results, a source was estimated below the 62-II crater at the depth of about 1 km.

In this study, whole InSAR processing was performed using SIGMA-SAR by Dr. Masanobu Shimada of JAXA-EROC. We used 10m-mesh Digital Elevation Model compiled by the Geospatial Information Authority of Japan (GSI). PALSAR level 1.0 data were provided from the Earthquake and Volcano Working Groups as well as PIXEL (PALSAR Interferometry Consortium to Study our Evolving Land surface) under a cooperative research contract with JAXA (Japan Aerospace Exploration Agency). The ownership of PALSAR data belongs to METI (Ministry of Economy, Trade and Industry) and JAXA.

Keywords: InSAR, Crustal Deformation, Tokachidake, ALOS, PALSAR, Volcano

Japan Geoscience Union Meeting 2012
(May 20-25 2012 at Makuhari, Chiba, Japan)

STT57-05 Room:201A Time:May 23 16:30-16:45

Analysis of crustal deformation due to the 2010 El Mayor-Cucapah Earthquake in Mexico using SAR data

OKAMOTO, Junichi[1*], HASHIMOTO, Manabu[1], FUKUSHIMA, Yo[1]

[1]DPRI, Kyoto University

El Mayor-Cucapah earthquake (Mw 7.2) occurred on April 4th, 2010, in Baja California, a region of high seismicity in association with the complex Pacific and North American plate boundary. Its hypocenter is located near a pull-apart basin and the tectonics in this area is very complex owing to distributed normal and conjugate strike-slip faults. In this study, we are going to reveal relationship between the generation process of co- and postseismic fault motions by detecting detailed co- and postseismic deformations by using ALOS/PALSAR and ENVISAT/ASAR data.

We detected range change of about 150cm in the vicinity of the source fault in the ascending co-seismic interferograms. However, we recognized disturbances of fringes in the vicinity of the northwestern part of the source fault and phase discontinuity at a separate fault off the main rupture. In the descending images, we can recognize many concentric fringes along the traces of northwestern part of the source fault, which suggest that local fault motion occurred in connection with the main rupture. In addition, the phase discontinuity is observed in the same area of the ascending interferograms. Therefore subsidiary faults off the main source fault may have generated local deformation during the main shock. We assumed a sufficiently large rectangular plane fault and estimated slip distributions on it. Right lateral strike slips with slight normal component were estimated, and its maximum slip of about 3.5m was obtained in the northwestern vicinity of the hypocenter and at a depth of 3-4km. The optimal dip angle was 68 degrees. While this model can explain the main feature of co-seismic deformation, the residuals in the vicinity of the northwestern part of the source fault are slightly larger than southeastern part. This suggests that it is difficult to explain these local deformations by estimated fault model.

During the postseismic period, about six months after the main shock, we recognized some signals in the northwestern part of the source fault in both ALOS and ENVISAT descending interferograms. Some profiles show range increases (movement to west or subsidence) up to 5cm. These displacements are observed on the west side of the source fault except at the northwestern edge. In addition, we recognized range increase of about 2.5cm in the vicinity of the other faults about 10km southwest of the source fault. This suggests that other faults, which did not slip during co-seismic period, could have moved during the postseismic period. We estimated postseismic slip distributions on the estimated co-seismic fault model. Reverse dip-slip components were dominant in the northwestern part. However this reverse dip-slip is inconsistent with slip during the mainshock in this region, and this model could not explain observed data well. Therefore observed postseismic deformations could have been generated by other factors.

Here, we assumed models with five faults dipping to southwest to explain the postseismic deformations. After trial and errors, we could find a model that can explain the observed phase variations and is consistent with co-seismic fault model which includes slightly normal component. This suggests that subsidiary faults in the vicinity of the source fault moved after the main shock as a result of complex changes of the stress in the crust.

Keywords: SAR, interferometry, El Mayor-Cucapah earthquake, coseismic deformation, postseismic deformation, afterslip

Japan Geoscience Union Meeting 2012
(May 20-25 2012 at Makuhari, Chiba, Japan)

STT57-06 Room:201A Time:May 23 16:45-17:00

2.5 Dimension Analysis of Ground Deformation in the Kyoto Basin and Osaka Plain Detected with SAR Interferometry

HASHIMOTO, Manabu[1*]

[1]DPRI, Kyoto University

We have been conducting an interferometry of SAR images acquired by ALOS/PALSAR and TerraSAR-X to reveal ground deformation and the configuration of basement of the Kyoto basin and the Osaka plain. We have analyzed PALSAR ascending images and applied a 2.5 dimension analysis to the stacked interferograms from both the ascending and descending orbits.

We analyzed 24 SAR images from the path 414 and frame 680 acquired during the period from October 8, 2006 to October 19, 2010. Pairs of images that have as short perpendicular baselines and long temporal intervals as possible were selected for interferometry. After that, interferograms were stacked to obtain average rate of line-of-sight (LOS) changes. During the interferometry, we applied flattening in order to reduce long-wavelength noise, which might have been originated by ionospheric disturbances. We used PALSAR images from descending orbit (path 65, frame 2920).

Last year, we detected LOS decrease in the southern part of Kyoto basin and LOS increase along the Arima-Takatsuki Tectonic Line (ATTL) from the analysis of descending images. Furthermore, analyses of TerraSAR-X images also gave similar results, which suggests that these observations revealed real ground deformations. In this study, we also recognized LOS decrease in southern part of Kyoto basin and LOS increase along the ATTL.

Then we applied 2.5 dimension analysis to these stacked interferograms to decompose LOS velocities in two directions into E-W and quasi-vertical components. Finally, we obtained about 1 cm/yr uplift in the southern part of Kyoto basin and 5 mm/yr subsidence along ATTL. In these areas, we did not recognize notable horizontal components, which suggests that they are purely uplift or subsidence. Interestingly, uplift in Kyoto is bounded by two active faults (Katagihara and Haibara faults). It is worth noting that more than 1 cm/yr subsidence were observed at the western edge of ATTL in the Toyonaka city. Other notable features are (1) subsidence in the reclaimed area on the coast of the Osaka Bay, (2) subsidence north of the Yodo River, and (3) subsidence west of the Osaka Prefectural Office.

The origin of these ground deformation remains hypothesis, but it is speculated that changes in groundwater table may affect the ground deformation in the Kyoto basin, since there is a big reservoir. Subsidence along ATTL may also be related to change in groundwater level and associated compaction of soil. One possibility is the postseismic effect of the 1995 Kobe earthquake, since the feature of the subsidence is quite similar to that observed during the postseismic period of the 2006 Mozambique earthquake.

PALSAR level 1.0 data were obtained from JAXA (Japan Aerospace Exploration Agency) under MEXT s (Ministry of Education, Culture, Sports, and Science and Technology) research project (Intensive Observation of the Uemachi Fault). The ownership of PALSAR data belongs to METI (Ministry of Economy, Trade and Industry) and JAXA. TerraSAR-X images were supplied by Pasco Ltd. under the Research Program by the Forum for the Application of SAR Technology. Copyright of TerreSAR-X images belongs to Infoterra GmbH.

Keywords: InSAR, ground deformation, Kyoto Basin, Osaka Plain, ground subsidence, Arima-Takatsuki Tectonic Line